MINIREVIEW

Check for updates

Recent development in halogen-bonding-catalyzed living radical polymerization

Chen-Gang Wang, [ID] Amerlyn Ming Liing Chong, Houwen Matthew Pan, Jit Sarkar, Xiu Ting Tay and Atsushi Goto [ID] *

Halogen bonding (XB) has been used to catalyze organic reactions and polymerizations, which is an emerging research area. Reversible complexation mediated polymerization (RCMP) is an XB-catalyzed living radical polymerization and is one of the most promising examples of the XB catalysis. RCMP utilizes alkyl iodides as initiating dormant species and electro-donating molecules and ions such as amines, iodide anions, and oxyanions as catalysts. Various initiating dormant species and catalysts were developed, enabling the synthesis of well-defined homopolymers and block copolymers with complex architectures, chain-end functionalization, photo-polymerization, and industrial application. The use of inexpensive non-metallic catalysts and the accessibility to a wide range of polymer structures are attractive features of RCMP. This mini-review summarizes the current research status of RCMP and its uniqueness brought *via* the XB catalysis.

1. Introduction

Halogen bonding (XB) is a noncovalent bond between an electron-accepting halogen (X) and an electron-donating base (B) (Fig. 1).[1] XB is a highly directional bond, and the R–X⋯B angle is close to 180°. The strength of XB increases in the order of X = F ≪ Cl < Br < I (with an increase in the polarizability of X) and with an increase in the electron-withdrawing ability of R. The B group can be electro-donating anions and neutral species such as halide anions, chalcogen- and pnictogen-containing species, and π-electron donors.[1,2] XB is widely utilized in crystal engineering,[2–4] supramolecular chemistry,[5–7] and functional materials such as luminescent crystals, porous frameworks, and conductive organic materials[8–12] due to its unique directionality, complementarity, and compatibility with various environments.

The application of XB has encompassed the creation of polymer materials. Similar to other non-covalent bonds, XB is used as an efficient driving force to form liquid-crystalline polymers, supramolecular gels, self-healing polymers, conjugated polymers, polymer nano-particles, phase separation structures, and polymer functional surfaces.[11–13] Resnati *et al.* reported a pioneering work on the preparation of liquid-crystalline comb-shaped polymers formed *via* the XB between poly(4-vinylpyridine) and α,ω-diiodoperfluoroalkanes in 2002.[14] XB

was also used to form supramolecular polymers using pyridine and iodopentafluorobenzene derivatives as molecular building blocks.[15] Steed *et al.* reported XB-bridged supramolecular gels using bis(pyridylurea) derivatives and 1,4-diiodotetrafluorobenzene.[16] Some XB-bridged supramolecular gels were stable in polar media such as aqueous methanol,[16] exhibiting the environmental compatibility of XB. Biomolecules bearing X and B moieties were used as building blocks to generate biomedical gels.[17] These examples demonstrate the usefulness of XB for the preparation of polymer materials.

XB was also used to form monomer (co)crystals. Polymers were synthesized *via* solid phase polymerizations of the monomer (co)crystals. Goroff *et al.* synthesized polyacetylenes *via* 1,4-addition polymerizations of diiodo-1,3-diacetylene (Fig. 2).[18,19] The co-crystal of diiodo-1,3-diacetylene (monomer) and bis(nitrile)oxalamide (XB linker) offered a high regularity of the monomer distance appropriate for topochemical polymerization (Fig. 2). Unlike the solution polymerization, where both 1,2- and 1,4-additions occur to generate branched irregular polymer structures, the topochemical polymerization in the crystal lattices predominantly led to 1,4-addition and afforded ordered polymer structures. Other examples of the

Division of Chemistry and Biological Chemistry, School of Physical and Mathematical Sciences, Nanyang Technological University, 21 Nanyang Link, 637371 Singapore. E-mail: agoto@ntu.edu.sg

Fig. 1 Halogen bonding.

Fig. 2 (a) Structures of 1,4-diiodo-1,3-butadiyne (monomer) and bis(4-cyanobutyl)oxalamide (XB linker). (b) X-ray structure of the co-crystal of the monomer and XB linker. (c) X-ray structure of the co-crystal of the obtained polymer (poly(diiododiacetylene)) and XB linker. Colours are as follows. C: gray; H: white; O: red; N: blue; I: magenta. Adapted with permission from ref. 18. Copyright 2006, American Association for the Advancement of Science.

solid-phase polymerizations of XB-based monomer (co)crystals are referred to excellent comprehensive reviews.[20,21]

Recently, solution-phase catalysis induced by XB has become an emerging area in organic synthesis.[22–24] XB induces an elongation of the R–X bond or a polarization of B, thereby catalysing organic reactions and polymerizations in solution phases. In organic chemistry, XB was used to activate less reactive substrates to achieve addition and cyclization reactions, for example.[25,26] On the other hand, only few examples on XB-catalyzed polymerization have been reported. Coulembier et al. reported an XB-catalyzed ring opening polymerization (ROP) of L-lactide (Scheme 1a) in 2010, in which iodine trichloride (catalyst) coordinates the monomer via XB and induces the polymerization.[27] Takagi et al. reported an XB-mediated living cationic polymerization of isobutyl vinyl ether (Scheme 1b) in 2017, in which 2-iodoimidazolium derivatives (catalysts) coordinate the alkyl halide dormant species via XB to generate a propagating carbon-centred cation.[28]
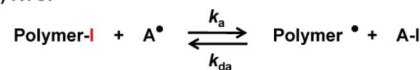

Scheme 1 XB-catalyzed (a) ring opening polymerization and (b) living cationic polymerization.

Scheme 2 Reversible activation: (a) general scheme in LRP, (b) RTCP, and (c) RCMP.

Living (or reversible-deactivation) radical polymerization (LRP) is a powerful technique for synthesizing well-defined polymers with narrow dispersities. Examples of the LRP systems are nitroxide-mediated polymerization (NMP),[29] atom transfer radical polymerization (ATRP),[30–32] reversible addition–fragmentation chain transfer (RAFT) polymerization,[33,34] iodine-transfer polymerization (ITP),[35] organotellurium-mediated radical polymerization (TERP),[36] and cobalt-mediated polymerization.[37] The basic concept of LRP is the reversible activation of a dormant species (polymer–X) to a propagating radical (polymer·) (Scheme 2a).[38]

Our research group developed organocatalyzed LRP systems using alkyl iodides as initiating dormant species and organic molecules as catalysts, which are reversible chain transfer catalyzed polymerization (RTCP) developed in 2006[39] and reversible complexation mediated polymerization (RCMP) developed in 2011.[40] RTCP and RCMP are mechanistically different, as described below, and RCMP uses XB catalysis. RCMP would be a good example highlighting the power of XB in polymer chemistry. In this mini-review, we summarize the recent development and applications of RTCP and RCMP with a particular focus on RCMP via XB catalysis. This mini-review refers particularly to our research for dedicating to the 2021 Polymer Chemistry Pioneering Investigators issue.

2. Polymerizations and applications

2.1. Mechanisms, catalysts, and typical polymerization behaviours of methyl methacrylate (MMA)

Both RTCP and RCMP use an alkyl iodide (R–I) as an initiating dormant species and an organic molecule as a catalyst. Mechanistically, RTCP uses a chain transfer between the dormant species and catalyst (Scheme 2b). RCMP uses an XB catalysis between the dormant species and catalyst (Scheme 2c).

An RTCP system consists of an R–I dormant species, a de-activator catalyst (A–I), and a conventional radical initiator such as an azo compound (Scheme 2b).[39] In RTCP, polymer[•], which is originally supplied by the conventional radical initiator, reacts with A–I, generating an activator radical (A[•]) as well as polymer–iodide (polymer–I). Subsequently, A[•] reversibly reacts with polymer–I to generate polymer[•] and A–I. This reversible chain transfer between the polymer and catalyst results in a reversible activation of polymer–I. A[•] radicals are germanium, phosphorus, nitrogen, oxygen, and carbon centred radicals, and examples of A–I are GeI$_4$, PI$_3$, and N-iodosuccinimide.[39,41–44]

An RCMP system consists of an R–I dormant species and an activator catalyst (Scheme 2c).[40] Polymer–I and the catalyst form an XB complex (polymer–I⋯catalyst), and the complex subsequently reversibly generates polymer[•] and an I[•]⋯catalyst complex. This reversible complexation mediates the polymerization, and hence the polymerization is termed RCMP. In organic chemistry, the reactions of alkyl halides (R–X) with amine bases (B) to generate the alkyl radicals via XB catalysis (R–X⋯B) have been well studied,[45–48] but the reactions were irreversible in all cases. Our research group found the reversible reactions using alkyl iodides, enabling the use of XB catalysis to LRP. Since our first report in 2011, we have developed several types of RCMP catalysts, including amines,[40,49] iodide anion (I^{−}),[50–54] organic superbases,[55] pseudohalide anions,[56] pyridine N-oxides,[57] and oxyanions[58] (Fig. 3). The reactivity of RCMP catalysts depends on their XB-forming ability, i.e., basicity or nucleophilicity, in principle. A representative catalyst is I^{−}. I^{−} is used in the form of salts such as tetrabutylammonium iodide (Bu$_4$N[+]I^{−}) (BNI).[50]

Fig. 4 (circles) show an example of RCMP of methyl methacrylate (MMA) (100 eq.) using iodo-2-methylpropionitrile (CP–I (Fig. 5a)) (1 eq.) as an initiating R–I and BNI (1 eq.) as an organic catalyst at 70 °C.[50] The number-average molecular weight (M_n) agreed with the theoretical value, and the dispersity ($Đ$) (= M_w/M_n) remained 1.1–1.2 throughout the polymerization, where M_w is the weight-average molecular weight. The M_n value was able to increase to 30 000 g mol^{-1} (Fig. 4 (triangles)) and up to 140 000 g mol^{-1} (ref. 50) with relatively small $Đ$ values (<1.5) for MMA.

The activation rate constant (k_a (Scheme 2c)) of PMMA–I with BNI was experimentally determined to be 0.050 M^{-1} s^{-1} in bulk MMA at 70 °C, where PMMA–I is poly(methyl methacrylate)–iodide.[50] This values mean that, with 80 mM of BNI (a typical catalyst concentration), PMMA–I is activated every 4 min, quantitatively confirming the high frequency of the catalytic activation and explaining why this RCMP system can provide low-dispersity polymers from an early stage of polymerization. In the I^{−} catalyst system, polymer–I is activated by I^{−} (activator) to generate polymer[•] and I$_2$[•−] (deactivator). I$_2$[•−] is not a stable radical and recombines with another I$_2$[•−] to generate I^{−} (activator) and I$_3$[−] (working as a deactivator).[50]

The free radical nature of the propagating species was supported by a radical trap experiment in low-mass model systems.[49–52,55–58] For example (Fig. 6a), an alkyl iodide CP–I (10 mM), an I^{−} catalyst (80 mM), and a radical trap 2,2,6,6-tetramethylpiperidinyl-1-oxy (TEMPO) (20 mM) were heated in a solvent at 60 °C.[50] If CP–I reacts with the catalyst to generate an alkyl radical CP[•], CP[•] is trapped by TEMPO, thereby yielding CP–TEMPO. Fig. 6a shows the ^{1}H NMR spectra before and after the heating. The signals (peaks a′, b′ and c′) of CP–

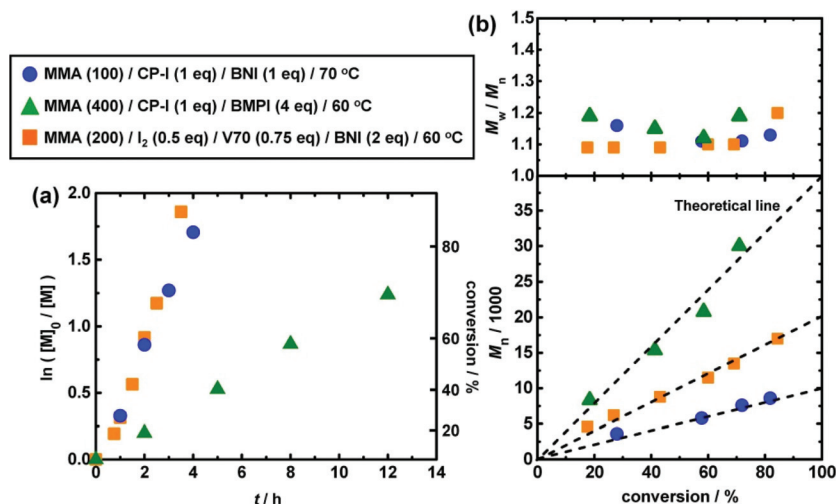Fig. 3   Structures and abbreviations of RCMP catalysts.

Fig. 4 Plots of (a) $\ln([M]_0/[M])$ *vs.* t and (b) M_n and M_w/M_n *vs.* conversion for RCMP of MMA. [M] is the concentration of monomer. The symbol and reaction conditions are indicated in the figure. V70 is 2,2'-azobis(4-methoxy-2,4-dimethylvaleronitrile). Adapted with permission from ref. 50. Copyright 2013, American Chemical Society.
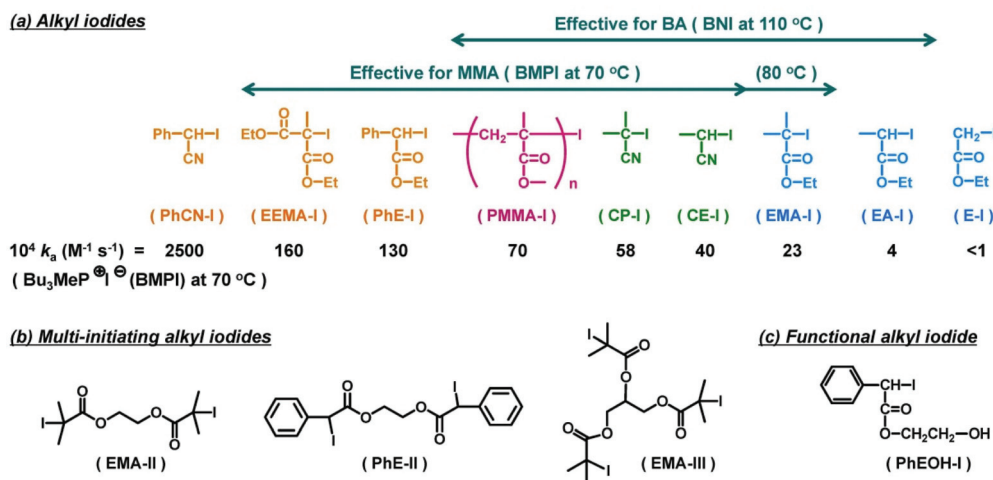

Fig. 5 Examples of R–I used in RCMP. (a) Mono-initiating alkyl iodides and the k_a values with tributylmethylphosphonium iodide (BMPI) in the toluene-d_8/acetonitrile-d_3 (90/10) mixture at 70 °C. The arrows indicate the ranges of effective alkyl iodides in the polymerizations of MMA and BA. (b) Multi-initiating alkyl iodides. (c) Functional alkyl iodide. Adapted with permission from ref. 60. Copyright 2014, American Chemical Society.

TEMPO was observed after the heating, proving the radical generation from CP–I.

The free radical nature of the propagating species was also confirmed from the tacticity of the polymer obtained in the polymerization of MMA with triethylamine as a catalyst.[40] The ^{13}C NMR spectrum (Fig. 6b)[40] showed that the pentad distribution (for the carbonyl carbon) is virtually the same as that for a conventional free radical polymerization. The polymerization was also completely inhibited in the presence of a radical trap TEMPO, supporting the radical mechanism during the polymerization.[40]

The XB complex (R–I···catalyst) formation was supported by a UV-Vis measurement in a low-mass model system containing CP–I as an alkyl iodide and tributylamine (TBA) as a catalyst.[49]

Fig. 6c shows the absorption spectra of TBA (80 mM) only, CP–I (80 mM) only, and a mixture of CP–I (80 mM) and TBA (80 mM) in bulk MMA. A new shoulder peak appeared for the mixture of CP–I and TBA at approximately 400 nm and ranged from 350 nm to 500 nm (solid line). The new peak would correspond to an XB complex of CP–I and TBA. Such red-shifted absorption was reported for complexes of alkyl chlorides/bromides with amines.[59]

Various alkyl iodides were used as initiating R–I dormant species (Fig. 5). Fig. 5a shows the k_a values of R–I with an I⁻ catalyst systematically determined in a polar solvent at 70 °C.[60] The k_a value tended to increase in the order of primary (E–I) < secondary (EA–I) < tertiary (EMA–I) alkyl groups, increase in the order of phenyl ≈ ester (EMA–I) < cyano (CP–I) stabilizing

Fig. 6 (a) ^{1}H NMR spectra (in the range of 0.5–2.5 ppm) of the solution of CP–I (10 mM), ethylmethyl imidazolium iodide (80 mM), and TEMPO (20 mM) heated at 60 °C for 0 and 15 h. The solvent was the mixture of toluene-d_8 and acetnitrile-d_3 (9 : 1). The mixture of toluene-d_8 (dielectric constant ε = 2.4) and acetonitrile-d_3 (ε = 37.5) is a model of MMA medium (ε = 7.9). (b) ^{13}C NMR spectrum (in the range of 175.5–179 ppm) of the polymer produced in the polymerization of MMA (100 eq.) with CP–I (1 eq.), triethylamine (0.5 eq.), and I$_2$ (1 eq.) at 90 °C for 3 h (monomer conversion = 76%, M_n = 7300, and Đ = 1.24). (c) UV-Vis spectra of TBA (80 mM) only (dotted line), CP–I (80 mM) only (dashed line), and a mixture of CP–I (80 mM) and TBA (80 mM) (solid line) in MMA (ambient temperature). Adapted with permission from ref. 40, 49, and 50. Copyright 2011 and 2013, American Chemical Society.

substituents, and increase in the order of one (EMA–I) < two (PhE–I) stabilizing substituents. Fig. 5a also depicts the range of effective R–I for the MMA and butyl acrylate (BA) polymerizations at different temperatures. In principle, an efficient R–I should have a sufficiently large k_a value, and also the released alkyl radical should be reactive enough for monomer addition. PhCN–I (Fig. 5a) releases a too stable alkyl radical and is not suitable for an initiating dormant species.

A possible drawback of RCMP is the use of R–I. Some alkyl iodides are not very stable for long-term storage. To address this issue, instead of an isolated R–I, an R–I generated *in situ* in the polymerization was also used. Molecular iodine (I$_2$) and an azo compound (R–N=N–R) were used as starting compounds, and for the polymerization, the R–I *in situ* formed was used. The I$_2$/azo method was originally developed by Lacroix-Desmazes *et al.* for ITP (reverse ITP (RITP))[35,61] and subsequently used in RCMP.[50,51] Fig. 4 (squares) shows the polymerization of MMA (200 eq.) with I$_2$ (0.5 eq.), an azo compound (2,2′-azobis(4-methoxy-2,4-dimethylvaleronitrile) (V70)) (0.75 eq.), and BNI (2 eq.) at 70 °C.[50] Virtually no polymerization occurred at 0.5 h, during which R–I was generated from I$_2$ and V70. After this period, the polymerization proceeded in a controlled manner. Another useful method to *in situ* generate R–I was a halogen exchange from the bromide precursors (R–Br) during the polymerization.[62–66]

2.2. Monomers and dispersity control

RCMP is amenable to a range of hydrophobic and hydrophilic functional methacrylates and also acrylates, styrene, and acrylonitrile (Fig. 7). The M_n value ranged from 10^3 to 10^5 g mol^{-1} and up to 290 000 g mol^{-1} with relatively small Đ values (<1.5).[50,67] Recently, RCMP was successfully used for biomass-derived itaconate derivatives (Fig. 7)[68] and biocompatible monomers (Fig. 7) such as 2-hydroxyethyl methacrylate
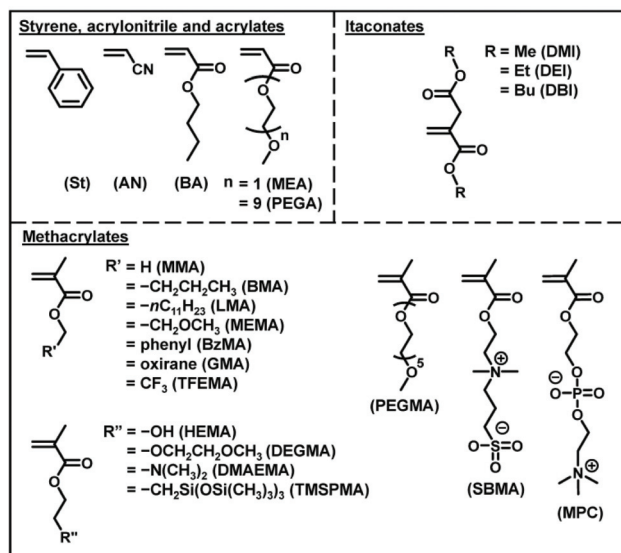

Fig. 7 Examples of the monomers applicable in RCMP.

(HEMA), poly(ethylene glycol) methyl ether methacrylate (PEGMA), 2-methoxyethyl acrylate (MEA), poly(ethylene glycol) methyl ether acrylate (PEGA), 2-methacryloyloxyethyl phosphoryl choline (MPC betaine monomer), and [2-(methacryloyloxy)ethyl]dimethyl-(3-sulfopropyl)ammonium hydroxide (SBMA betaine monomer).[52] Green RCMP systems of such biocompatible monomers using biocompatible catalysts such as choline iodide analogues (AChI and BChI (Fig. 3)) and carboxylates (NaFum and TMGL (Fig. 3)) and non-toxic solvents such as ethyl lactate, ethanol, and water were also developed, being attractive for sustainable society.[52,58]

Hunter *et al.* reported that the stability of XB is relatively insensitive to the solvent polarity.[69] The association constant

of an I_2/urea XB complex ([complex]/([I_2][urea])) decreased by only one order of magnitude by changing the solvent from alkanes (*n*-octane) to alcohols (methanol), for example. The solvent-insensitivity of XB is in sharp contrast to the significant solvent-sensitivity of hydrogen bonding. The stability (association constant) of a phenol/urea hydrogen bonding complex decreased by as much as three orders of magnitude by changing the solvent from *n*-octane to methanol. This weak sensitivity of XB to reaction media would rationalize the amenability of RCMP to a wide range of hydrophobic and hydrophilic monomers and solvents.

Catalytic monomers containing a polymerizable methacrylate or acrylate moiety and a catalytic quaternary ammonium iodide (QAI) moiety were developed as a new type of monomers.[53] The catalytic function incorporated in the monomer enabled a self-catalysed RCMP. Also interestingly, the obtained polymers bore QAI moieties at the side chains and may be used for antibacterial applications.

The dispersity ($Đ$) is an important parameter determining polymer properties such mechanical strength, miscibility, stimuli-responsive transition, and self-assemble behavior.[70,71] Thus, the modulation of the $Đ$ value is an emerging interest in polymer chemistry.[71–76] RCMP was also used to modulate the $Đ$ value exploiting a unique temperature-selective activation of polymer–I (Fig. 8a).[77] The RCMP of a methacrylate was conducted in the presence of a small amount of an acrylate (4–10%) at a mild temperature of 60 °C. At this mild temperature, the RCMP of the methacrylate smoothly proceeded, but once the dormant polymer chain contained an acrylate at the terminal unit, the chain was hardly activated because of its strong carbon–iodide bond. Thus, the acrylate-terminal chain accumulated over the polymerization, thus increasing the $Đ$ value (Fig. 8a). The $Đ$ value was finely tuned by varying the amount of the acrylate. Importantly, such an acrylate-terminal dormant chain was not a dead polymer but was able to be re-

activated at an elevated temperature of 110 °C (Fig. 8b), enabling the synthesis of di-block, multi-block, star-shaped, and brush-shaped block copolymers with tailored $Đ$ values.

2.3. Polymers with complex architectures

RCMP can yield polymer–I with high degrees of iodide-chain-end fidelity (livingness) (92–99% with ±5% experimental error) up to relatively high monomer conversions (*e.g.*, a 78% monomer conversion).[50] Such high iodide-chain-end fidelity allows efficient block copolymerizations and chain-end modifications. RCMP was used to synthesize a range of di-block, tri-block, and multi-block copolymers[78–80] and polymers with complex architectures such as star polymers[51,78,81] and hyper-branched copolymers.[82,83] Tri-block copolymers were synthesized from alkyl di-iodides with two initiating moieties (Fig. 5b).[78] For example, PMMA-*b*-PBA-*b*-PMMA and PBA-*b*-PMMA-*b*-BA with different (ABA and BAB) sequences were obtained, where PBA is poly(butyl acrylate). 3-Arm star polymers were synthesized from an alkyl tri-iodide (Fig. 5b).[78] Hyper-branched polymers were synthesized using an inimer containing a polymerizable vinyl group and an alkyl iodide moiety.[83]

A temperature-selective radical generation from a designed alkyl di-iodide (I–R^2–R^1–I) initiator, 2-iodo-2-(4′-(2″-iodopropionyloxy)phenyl-acetate) (I–MEPE–I) (Fig. 9), opened up the synthesis of asymmetric CABC tetra-block copolymers.[79] The reactivities of I–R^2 and R^1–I were largely different; R^1–I initiated at a mild temperature (60 °C) and I–R^2 initiated only at an elevated temperature (110 °C). Methacrylates A and B were polymerized from the R^1–I (PE–I) site at 60 °C, at which temperature the I–R^2 (I–ME) site remained unreacted (Fig. 9). Subsequently, an acrylate C was polymerized at 110 °C, at which temperature the polymerization occurred from both

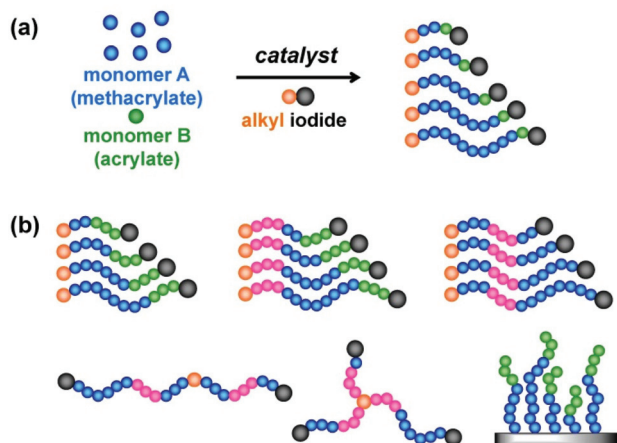Fig. 8 (a) One-pot synthesis of polymer with high dispersity and high iodide chain-end fidelity. (b) Applications to various types of block copolymers. Adapted with permission from ref. 77. Copyright 2019, John Wiley and Sons.

Fig. 9 Temperature-selective initiation from I–MEPE–I for the synthesis of CABC tetra-block copolymer. Adapted with permission from ref. 79. Copyright 2018, John Wiley and Sons.

chain ends, yielding asymmetric CABC tetra-block copolymers (Fig. 9). The temperature-selective radical generation was further exploited for the synthesis of ABC-type miktoarm star copolymers.[81]

Polymer–I was used as a macroinitiator to synthesize di-block copolymers. When polymer–I is a polymethacrylate–iodide, owing to the weak carbon–iodide bond, polymer–I is sometimes not very stable upon long-term storage. To address this issue, a PMMA containing an unsaturated chain-end (PMMA–Y) was used as a macroinitiator to synthesize block copolymers, where Y is $CH_2C(=CH_2)COOCH_3$.[84,85] PMMA–Y was converted to PMMA• via an addition fragmentation chain transfer (AFCT), and the generated PMMA• was used for the block polymerization via RCMP, yielding block copolymers. The use of PMMA–Y as a macroinitiator is a convenient method to obtain block copolymers.

2.4. Chain-end functionalization

Chain-end functionalized polymers are of great interest for their use as building blocks to create architecturally designed polymers or to graft on solid surfaces for surface modification.[86,87] The use of functional R–I initiators (Fig. 5c) in RCMP provided polymers with functional groups at the initiating chain end.[51,61] Another approach was the post iodide-chain-end transformation of polymer–I, providing polymers with functional groups at the growing chain end. The weak carbon–iodide bond facilitated the chain-end transformation.

For polyacrylates, polymer–I was reacted with primary amines (NH_2R), successfully generating polymers (polymer–NHR) with, e.g., phenyl, alkyl, OH, NH_2, SH, and $Si(OEt)_3$ functionalities at the R moiety.[88] A photo-selective chain-end transformation of polymer–I was conducted using bifunctional cysteamine ($NH_2CH_2CH_2SH$) (Fig. 10a).[89] Without photo irradiation, the chain-end iodide reacted with the amino group of cysteamine to generate a thiol-terminated polymer (polymer–SH) (Fig. 10c). With UV irradiation, the carbon–iodide bond was homolytically cleaved to give a carbon-centred radical (polymer•), which subsequently underwent a radical chain transfer with the thiol group of cysteamine to generate a hydrogen-terminated polymer (polymer–H) (Fig. 10c). Thus, by switching the UV irradiation on and off, polymer–H and polymer–SH were selectively obtained from the same reactants (polymer–I and cysteamine). Another photo-selective chain-end transformation of polymer–I was conducted co-using NH_2R and formic acid (Fig. 10b), which widened the scope of the chain-end functionality.[90] Without photo irradiation, polymer–I reacted with NH_2R to generate polymer–NHR with, e.g., phenyl, alkyl, OH, NH_2, SH, and $Si(OEt)_3$ functionalities at the R moiety, while with UV irradiation, polymer–I was converted to polymer–H via a photochemical reaction with formic acid (Fig. 10c).

Pseudo-halide anions such azide (N_3^-), thiocyanate (SCN^-), and cyanate (OCN^-) anions form XB with polymer–I and are good catalysts of RCMP. Interestingly, the reactions of polymer–I with the pseudo-halide anions were solvent-selective.[56] In non-polar solvents, N_3^- served as a catalyst for polymer–I to reversibly generate polymer•. In polar solvents, N_3^- worked as a nucleophile for polymer–I to undergo a substitution reaction generating an azide chain-end functionalized polymer–N_3. Exploiting this solvent selectivity, one-pot synthesis of azide chain-end PMMA (PMMA–N_3) was conducted; namely, the RCMP of MMA with sodium azide (NaN_3) was conducted in a non-polar solvent to generate PMMA–I, and subsequently to the same reaction solution, a polar solvent was added to convert PMMA–I to PMMA–N_3 in one-pot.

Tetrabutylammonium azide (BNN_3) was also used instead of NaN_3.[91] Different from NaN_3, BNN_3 led to the substitution even in non-polar solvents. This feature enabled the post-azidation of fluorinated (super-hydrophobic) polymer–I in non-polar solvents, which are otherwise insoluble in polar solvents. Azide chain-end polymers are highly useful to construct complex macromolecules through a click reaction.[92]

2.5. Photo-polymerization

Photo-controlled LRPs have widely been explored.[93–96] Photo-controlled ATRP and RAFT polymerization using organic catalysts are emerging techniques attracting great attention.[97–102] Photo-controlled RCMP (photo-RCMP) uses an initiating R–I and a light-absorbing organic catalyst.[49,103] A possible mechanism (Fig. 11) is that the catalyst coordinates polymer–I to form the polymer–I···catalyst complex and that the catalyst serves as an antenna to absorb the light. The energy is subsequently transferred from the catalyst to the C–I bond, giving rise to the C–I cleavage. Notably, several organic molecules with different absorption wavelengths were feasible, covering the entire visible light region (350–750 nm) (Fig. 11).[103] The polymerization was also an ideal on–off switchable system with and without the light irradiation. An application was a one-pot selective regulation of RCMP and another type of
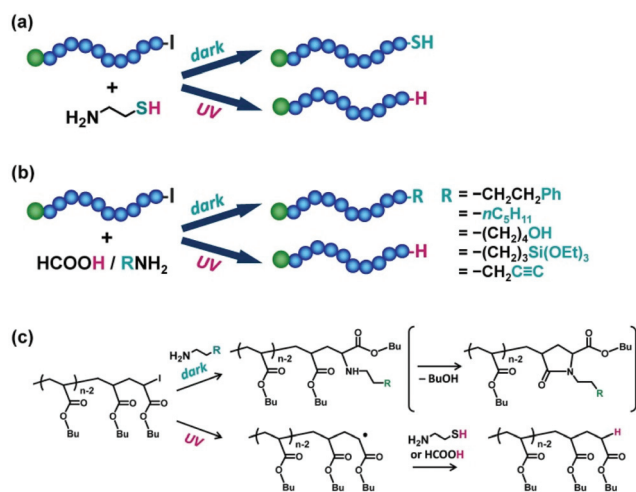
Fig. 10 Photo-selective chain-end functionalization with (a) cysteamine and (b) primary amines and formic acid and (c) the mechanisms. Adapted with permission from ref. 89 and 90. Copyright 2018 and 2019, Royal Society of Chemistry.

Fig. 11 Possible mechanism for photo-RCMP and photo-catalysts. Adapted with permission from ref. 103. Copyright 2015, American Chemical Society.

polymerization (ring opening polymerization (ROP)) (Scheme 3). Using different irradiation wavelengths (550–750 nm for RCMP and 350–380 nm for ROP), the polymerizations of MMA and δ-valerolactone (VL) were initiated and controlled from a dual initiator of RCMP and ROP in one-pot, generating a block copolymer of MMA and VL.[103]

Zhang, Cheng, and coworkers developed visible-light-controlled RCMP systems. One system used polar solvents such as dimethyl sulfoxide as catalysts to form the polymer–I⋯solvent complex.[104] Another system used amine-functional monomers as catalytic monomers to form the polymer–I⋯monomer complex.[105] Both systems were driven *via* visible-light irradiation using LEDs or natural sunlight. Near-infrared (NIR)-controlled RCMP was achieved using the polymer–I⋯(carbonyl compound) complex.[106] The high-penetration of the NIR light enabled the successful polymerizations even through thick barriers such as pork skin and A4 paper between the light source and the polymerization solution. Water was also used as a catalyst to form the polymer–I⋯water complex under blue-LED irradiation.[107] Li *et al.* demonstrated the *in situ* bromide–iodide transformation of the initiator and the subsequent photo-RCMP, both of which were controlled by white-LED irradiation.[108] Matyjaszewski *et al.* showed the successful

Scheme 3 Synthesis of poly(methyl methacrylate)-*b*-poly (δ-valerolactone) block copolymer *via* photo-polymerization. Adapted with permission from ref. 103. Copyright 2015, American Chemical Society.

iodine-mediated photo ATRP in aqueous media with oxygen tolerance under visible light irradiation, offering a green and highly efficient photo polymerization.[66]

2.6. Heterogeneous polymerization and self-assembly

RTCP and RCMP were not only conducted in homogeneous (bulk and solution) systems but also in heterogeneous systems. The first report was an aqueous microsuspension RTCP of MMA using CP–I (R–I initiator), *N*-iodosuccinimide (NIS) (catalyst), and *n*-tetradecyltrimethyl ammonium bromide (surfactant), in which a high monomer conversion (93%) was attained within 2 h.[109] Instead of water, supercritical carbon dioxide was also used in a dispersion RTCP of styrene, giving relatively small Đ values (1.3–1.5).[110]

Amphiphilic block copolymers can self-assemble in selective solvents. The obtained micelles, worms, vesicles, and other structures are widely utilized as delivery containers, nano-reactors, and imaging materials, for example.[111] Such self-assemblies can be obtained using pre-synthesized block copolymers or obtained during block polymerizations, the latter of which is known as polymerization induced self-assembly (PISA).[112–116] A significant advantage of PISA is the high polymer concentration (solid content) attainable in the reaction mixture. In PISA, a macroinitiator, which is soluble in the solvent, undergoes chain-extension with another monomer to generate an amphiphilic block copolymer. During the polymerization, as the second block (solvent-insoluble) segment grows, the block copolymer becomes insoluble in the solvent, *in situ* generating self-assemblies.

The combination of PISA with RCMP provided micelles, worms, and vesicles.[64,117,118] Fig. 12 shows the morphology diagram in a PISA using PMAA and PMMA as hydrophilic and hydrophobic segments, respectively, where PMAA is poly (methacrylic acid).[117] The assembly structure shifted from micelles to worms and vesicles with an increase in the fraction of the hydrophobic PMMA segment in the block copolymer. A biocompatible poly(poly(ethylene glycol) methyl ether methacrylate) (PPEGMA) was also used as a hydrophilic segment, forming micelles and vesicles with biocompatible surfaces.[118] The encapsulation of an external molecule was also tested.[118] Instead of thermal RCMP, Zhu *et al.* utilized photo-RCMP in a PISA of benzyl methacrylate under blue LED light, successfully obtaining micelles, worms, and vesicles.[64] RCMP is free from sulfur and transition metals. The obtained nano-particles and nano-capsules may be useful for biomedical, cosmetic, and agrochemical applications.

Pre-synthesized block copolymers *via* RCMP were also used to obtain self-assemblies. Amphiphilic CABC tetra-block copolymers (section 2.3) gave unique particles such as Janus-type star particles and flower-like particles, depending on the A, B, and C segments (Fig. 13).[79,80,119] Interestingly, the Janus-type star particle contains dual cores and may serve as a dual container of two different guest molecules in a co-delivery system (Fig. 13). The use of a thermo-responsive polymer in the C segment enabled reversible transformation between the star and flower (Fig. 13), which was used in encapsulation and
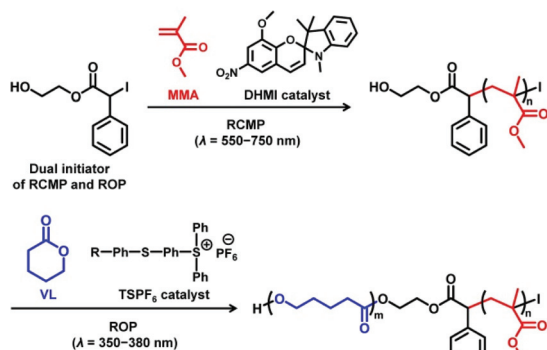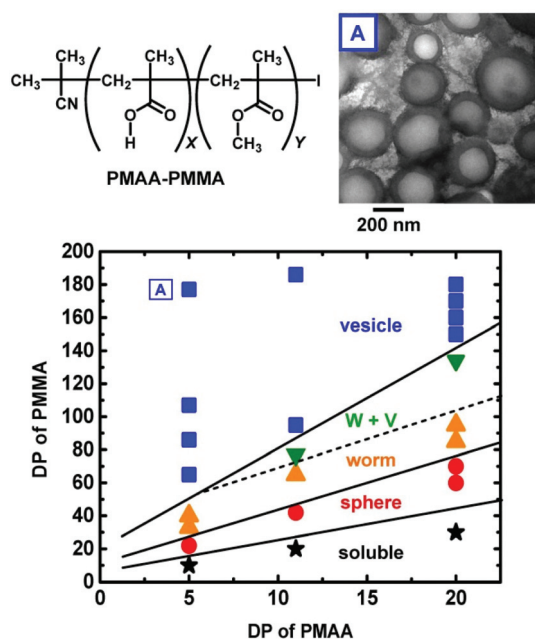
Fig. 12 Morphology diagram of the self-assemblies generated in the PISA process for PMAA–PMMA in ethanol, structure of PMAA–PMMA, and TEM image of vesicle. The solid content was 5–9 wt%. W + V denotes a mixture of worms and vesicles. DP is the degree of polymerization. Adapted with permission from ref. 117. Copyright 2018, Royal Society of Chemistry.
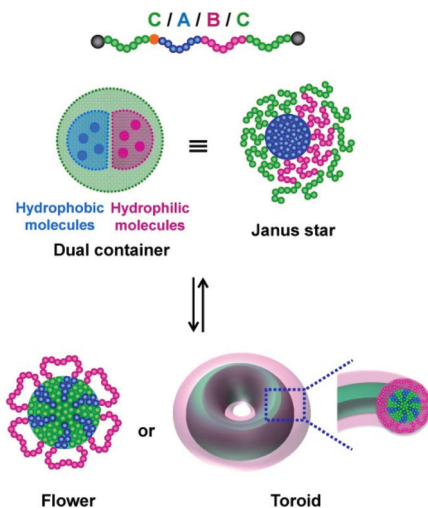

Fig. 13 (a) Reversible morphological transformation between Janus star micelle and flower micelle or toroid using CABC tetra-block copolymer. Adapted with permission from ref. 75. Copyright 2020, John Wiley and Sons. Adapted with permission from ref. 119. Copyright 2020, Royal Society of Chemistry.

release of guest molecules and temperature-dependent shielded and exposed functional surfaces.[80] Not only the flower but also discs, toroids, and a porous structure were also obtained.[119] Besides CABC tetra-block copolymers, an amphiphilic star polymer with three different arms formed a large

compound micelle,[81] and an amphiphilic rod-coil di-block copolymer yielded micelles and vesicles.[68]

2.7. Polymer brushes

Surface-initiated LRP (LRP from surface-bound initiators) is an enabling technique for fabricating concentrated polymer brushes on solid surfaces.[120–122] Patterned polymer brushes are of interest because polymer brushes with different physical properties are spatially arranged.[123,124] Patterned polymer brushes find applications to bio-microarray, molecular recognition, and microelectronic devices, for example.[124]

Polymer brushes were obtained *via* thermal surface-initiated RTCP[78] and RCMP.[125] Patterned polymer brushes were obtained *via* photo-controlled surface-initiated RCMP (photo-SI-RCMP).[125] Positive-type patterned brushes were prepared *via* photo-SI-RCMP under visible light (500–600 nm) using photomasks (Fig. 14a). Negative-type patterned brushes were also prepared (Fig. 14b). The R–I initiator carries a weak carbon–iodide bond and could be degraded very rapidly (within 1 min) under UV light (250–385 nm). The degradation of the R–I initiator was conducted under UV light using photo-
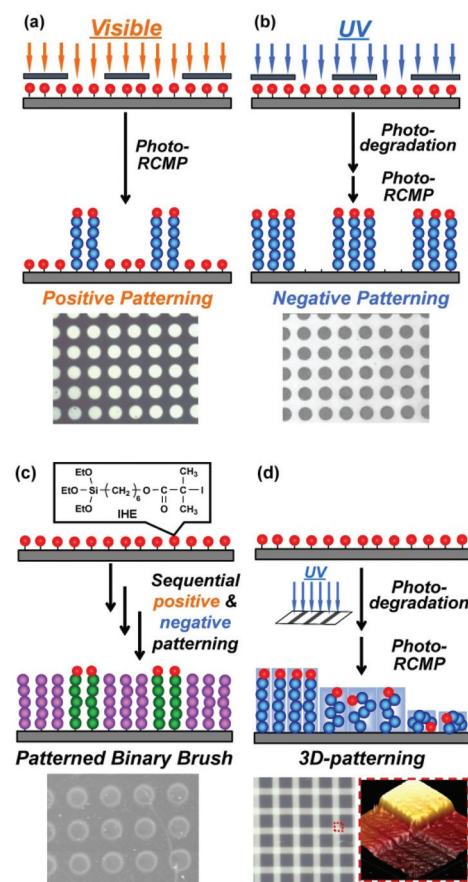

Fig. 14 (a) Positive-type patterned brush. (b) Negative-type patterned brush. (c) Patterned binary brush. (d) 3D-patterning with different graft density. Adapted with permission from ref. 125. Copyright 2018, John Wiley and Sons. Adapted with permission from ref. 67. Copyright 2019, American Chemical Society.

masks, and the subsequent photo-SI-RCMP under visible light generated negative-type patterned brushes (Fig. 14b). Sequential combination of the positive and negative patterning afforded complex patterned brushes such as patterned binary brushes (Fig. 14c) and patterned block copolymer brushes.[125] The graft density of polymer brush was also tailored by adjusting UV-irradiation energy in the initiator degradation step, by which three-dimensional (3D) patterned brushes with high-density (concentrated), moderate-density (semi-diluted), and low-density (diluted) brush areas were prepared (Fig. 14d).[67] The size exclusion of external molecules from the polymer brush depends on the graft density.[122] Thus, the patterned brushes with different graft densities may serve as molecular recognition interfaces. Patterned cross-linked polymer brushes were also prepared.[126] Crosslinking and decrosslinking were reversibly triggered by thermal, chemical, and photo stimuli, which was used to modulate the surface wettability and create and delete the brush patterns.

Polymer brushes with patterned chain-end functionalities were also prepared. The brush chain-end iodide was converted to thiol, alkyne, and hydrogen in patterned manners using photo-selective reactions (section 2.4) with photomasks.[89,90] The thiol chain-end was further labelled with a fluorescent maleimide *via* a thiol–maleimide click reaction, giving patterned fluorescent brushes,[89] and the alkyne chain-end was copolymerized with a fluorinated vinyl monomer, giving refractive-index patterned brushes.[90]

2.8. Application in industry

Dainichiseika Color & Chemicals Mfg. Co., Ltd has commercially used RTCP/RCMP for manufacturing block copolymers at industrial scales (Fig. 15). They use the block copolymers as dispersants of pigments for printer inks and other applications. RTCP and RCMP use relatively inexpensive initiators and catalysts and are free from metals and odour, serving as a cost-effective manufacturing process. Various R–I initiators are available from Godo Shigen Co., Ltd. Some R–I initiators are also available from Tokyo Chemical Industry (TCI) Co., Ltd.

2.9. Solid-phase polymerization

Solid-phase polymerization (SPP) of solid monomer (co) crystals is widely used in polymer synthesis.[127–130] As mentioned, the use of XB-based monomer (co)crystals in topochemical SPP enabled the synthesis of structurally controlled polymers.[20,21] Recently, XB-based monomer co-crystals were for the first time used in free radical SPP.[131] Because hydrogen bonding had almost predominantly been used to obtain monomer (co)crystals for free radical SPP, the use of XB widened the monomer scope for free radical SPP (encompassing monomers without hydrogen bonding moieties). The XB-based monomer co-crystals were prepared using electron-donating monomers such as vinyl pyridine and an electron-accepting linker (1,4-diiodotetrafluorobenzene) (Fig. 16). The monomers were regularly aligned in the crystals, and the adjacent vinyl groups were close enough to undergo chain propagation. Free radical SPP was conducted thermally and photochemically, yielding polymers with large M_n values and small $Đ$ values because of the monomer alignment in the crystals. Interestingly, liquid monomers (*e.g.*, vinyl pyridine) were converted to solid monomer co-crystals before the polymerization (Fig. 16). This feature enabled the construction of pre-shaped desired architectures such as sheets before the polymerization, and the architectures were fixed *via* SPP (Fig. 16). Complex architectures such as a 3D-shaped architecture and a layered sheet actuator were also obtained. This approach may serve as a useful polymer engineering tool for using liquid monomers to constitute pre-determined polymer material architectures.

Fig. 15 Dispersion of pigment nano-particles using block copolymers and pilot reactor for industrial manufacturing in Dainichiseika Color & Chemicals Mfg. Co., Ltd.

Fig. 16 XB-based monomer co-crystal and SSP. Adapted with permission from ref. 131. Copyright 2020, John Wiley and Sons.

3. Conclusions and outlook

Because of the abundance of XB synthons, high complementarity, and compatibility in polar and nonpolar environments, XB offers useful catalytic reactions. RCMP would be one of the most promising examples of XB-catalysis. RCMP is attractive in its broad monomer scope, accessibility to a range of polymer structures, mild polymerization conditions, and absence of metals and odour. The catalysts encompassed amines, iodide anions, pseudo-halide anions, and oxygen-centred anions. Various block copolymers and branched polymers were obtained using designed R–I initiators. The post-transformation of the chain-end iodide offered various chain-end functionalized polymers. Polymer nanoparticles and (patterned) polymer brushes were accessed *via* heterogeneous and photo-controlled polymerizations. Besides RCMP, free-radical SPP of XB-based monomer co-crystals provided pre-shaped polymer material architectures using liquid monomers.

Like other XB catalysis, RCMP can use organic compounds as catalysts. The use of non-metal, less toxic, and colorless catalysts would be attractive in electronic, biomedical, and optical applications. I^-, pseudo-halide anion, and oxyanion catalysts are used in the form of organic salts such as $Bu_4N^+I^-$ or alkali metal salts such as Na^+I^-. Na^+ is not a heavy metal and is still biologically safe. A possible drawback of RCMP is the use of R–I initiators, some of which gradually degrade upon long-term storage. The use of the R–I *in situ* generated *via*, *e.g.*, the I_2/azo method and halogen exchange would be a possible solution. As a future direction, further development of efficient catalysts and use of environmental–friendly conditions are important for widened applications and sustainable society. Such efficient catalysts are desired to expand the monomer scope, molecular weight range, and accessible polymer structures. The use of environmentally–friendly catalysts and solvents and also the development of robust processes for the removal of catalysts and chain-end iodide from the product polymers would further increase the feasibility of RCMP for industrial use. This mini-review summarised the state-of-the-art of RCMP. We hope that the mini-review will be helpful for further exploration of XB catalysis and further development of RCMP.

Conflicts of interest

There are no conflicts to declare.

Acknowledgements

References

1   G. Cavallo, P. Metrangolo, R. Milani, T. Pilati, A. Priimagi, G. Resnati and G. Terraneo, *Chem. Rev.*, 2016, **116**, 2478–2601.

2   M. K. Corpinot and D.-K. Bučar, *Cryst. Growth Des.*, 2019, **19**, 1426–1453.

3   A. Mukherjee, S. Tothadi and G. R. Desiraju, *Acc. Chem. Res.*, 2014, **47**, 2514–2524.

4   J.-C. Christopherson, F. Topić, C. J. Barrett and T. Friščić, *Cryst. Growth Des.*, 2018, **18**, 1245–1259.

5   P. Metrangolo, F. Meyer, T. Pilati, G. Resnati and G. Terraneo, *Angew. Chem., Int. Ed.*, 2008, **47**, 6114–6127.

6   L. C. Gilday, S. W. Robinson, T. A. Barendt, M. J. Langton, B. R. Mullaney and P. D. Beer, *Chem. Rev.*, 2015, **115**, 7118–7195.

7   M. J. Langton, C. J. Serpell and P. D. Beer, *Angew. Chem., Int. Ed.*, 2016, **55**, 1974–1987.

8   F. Meyer and P. Dubois, *CrystEngComm*, 2013, **15**, 3058–3071.

9   B. Li, S.-Q. Zang, L.-Y. Wang and T. C. W. Mak, *Coord. Chem. Rev.*, 2016, **308**, 1–21.

10 J.-C. Christopherson, F. Topić, C. J. Barrett and T. Friščić, *Cryst. Growth Des.*, 2018, **18**, 1245–1259.

11 M. Saccone and L. Catalano, *J. Phys. Chem. B*, 2019, **123**, 9281–9290.

12 G. Berger, P. Frangville and F. Meyer, *Chem. Commun.*, 2020, **56**, 4970–4981.

13 G. Berger, J. Soubhye and F. Meyer, *Polym. Chem.*, 2015, **6**, 3559–3580.

14 R. Bertani, P. Metrangolo, A. Moiana, E. Perez, T. Pilati, G. Resnati, I. Rico-Lattes and A. Sassi, *Adv. Mater.*, 2002, **14**, 1197–1201.

15 J. Xu, X. Liu, T. Lin, J. Huang and C. He, *Macromolecules*, 2005, **38**, 3554–3557.

16 L. Meazza, J. A. Foster, K. Fucke, P. Metrangolo, G. Resnati and J. W. Steed, *Nat. Chem.*, 2013, **5**, 42–47.

17 A. Bertolani, L. Pirrie, L. Stefan, N. Houbenov, J. S. Haataja, L. Catalano, G. Terraneo, G. Giancane, L. Valli, O. Ikkala, G. Resnati and P. Metrangolo, *Nat. Commun.*, 2015, **6**, 7574.

18 A. Sun, J. W. Lauher and N. S. Goroff, *Science*, 2006, **312**, 1030–1034.

19 C. Wilhelm, S. A. Boyd, S. Chawda, F. W. Fowler, N. S. Goroff, G. P. Halada, C. P. Grey, J. W. Lauher, L. Luo, C. D. Martin, J. B. Parise, C. Tarabrella and J. A. Webb, *J. Am. Chem. Soc.*, 2008, **130**, 4415–4420.

20 K. Biradha and R. Santra, *Chem. Soc. Rev.*, 2013, **42**, 950–967.

21 A. Chaudhary, A. Mohammad and S. M. Mobin, *Cryst. Growth Des.*, 2017, **17**, 2893–2910.

22 R. L. Sutar and S. M. Huber, *ACS Catal.*, 2019, **9**, 9622–9639.

23 J. Bamberger, F. Ostler and O. G. Mancheño, *ChemCatChem*, 2019, **11**, 5198–5211.

24 D. Bulfield and S. M. Huber, *Chem. – Eur. J.*, 2016, **22**, 14434–14450.

25 J.-P. Gliese, S. H. Jungbauer and S. M. Huber, *Chem. Commun.*, 2017, **53**, 12052–12055.

26 A. Dreger, P. Wonner, E. Engelage, S. M. Walter, R. Stoll and S. M. Huber, *Chem. Commun.*, 2019, **55**, 8262–8265.

27 O. Coulembier, F. Meyer and P. Dubois, *Polym. Chem.*, 2010, **1**, 434–437.

28 K. Takagi, K. Yamauchi and H. Murakata, *Chem. – Eur. J.*, 2017, **23**, 9495–9500.

29 J. Nicolas, Y. Guillaneuf, C. Lefay, D. Bertin, D. Gigmes and B. Charleux, *Prog. Polym. Sci.*, 2013, **38**, 63–235.

30 K. Matyjaszewski and N. V. Tsarevsky, *J. Am. Chem. Soc.*, 2014, **136**, 6513–6533.

31 K. Matyjaszewski, *Adv. Mater.*, 2018, **30**, 1706441.

32 M. Ouchi and M. Sawamoto, *Macromolecules*, 2017, **50**, 2603–2614.

33 D. J. Keddie, G. Moad, E. Rizzardo and S. H. Thang, *Macromolecules*, 2012, **45**, 5321–5342.

34 S. Perrier, *Macromolecules*, 2017, **50**, 7433–7447.

35 G. David, C. Boyer, J. Tonnar, B. Ameduri, P. Lacroix-Desmazes and B. Boutevin, *Chem. Rev.*, 2006, **106**, 3936–3962.

36 S. Yamago, *Chem. Rev.*, 2009, **109**, 5051–5068.

37 A. Debuigne, R. Poli, C. Jerome, R. Jerome and C. Detrembleur, *Prog. Polym. Sci.*, 2009, **34**, 211–239.

38 A. Goto and T. Fukuda, *Prog. Polym. Sci.*, 2004, **29**, 329–385.

39 A. Goto, H. Zushi, N. Hirai, T. Wakada, Y. Tsujii and T. Fukuda, *J. Am. Chem. Soc.*, 2007, **129**, 13347–13354.

40 A. Goto, T. Suzuki, H. Ohfuji, M. Tanishima, T. Fukuda, Y. Tsujii and H. Kaji, *Macromolecules*, 2011, **44**, 8709–8715.

41 A. Goto, Y. Tsujii and T. Fukuda, *Polymer*, 2008, **49**, 5177–5185.

42 A. Goto, N. Hirai, T. Wakada, K. Nagasawa, Y. Tsujii and T. Fukuda, *Macromolecules*, 2008, **41**, 6261–6264.

43 A. Goto, N. Hirai, K. Nagasawa, Y. Tsujii, T. Fukuda and H. Kaji, *Macromolecules*, 2010, **43**, 7971–7978.

44 P. Vana and A. Goto, *Macromol. Theory Simul.*, 2010, **19**, 24–35.

45 D. P. Stevenson and G. M. Coppinger, *J. Am. Chem. Soc.*, 1962, **84**, 149–152.

46 H. Ishibashi, S. Haruki, M. Uchiyama, O. Tamura and J. Matsuo, *Tetrahedron Lett.*, 2006, **47**, 6263–6266.

47 F. Sladojevich, E. McNeill, J. Bcrgel, S.-L. Zheng and T. Ritter, *Angew. Chem., Int. Ed.*, 2015, **54**, 3712–3716.

48 Y. Wang, J. Wang, G.-X. Li, G. He and G. Chen, *Org. Lett.*, 2017, **19**, 1442–1445.

49 A. Ohtsuki, A. Goto and H. Kaji, *Macromolecules*, 2013, **46**, 96–102.

50 A. Goto, A. Ohtsuki, H. Ohfuji, M. Tanishima and H. Kaji, *J. Am. Chem. Soc.*, 2013, **135**, 11131–11139.

51 J. Sarkar, L. Xiao and A. Goto, *Macromolecules*, 2016, **49**, 5033–5042.

52 C.-G. Wang, F. Hanindita and A. Goto, *ACS Macro Lett.*, 2018, **7**, 263–268.

53 C.-G. Wang, X. Y. Oh, X. Liu and A. Goto, *Macromolecules*, 2019, **52**, 2712–2718.

54 C.-G. Wang, J. J. Chang, E. Y. J. Foo, H. Niino, S. Chatani, S. Y. Hsu and A. Goto, *Macromolecules*, 2020, **53**, 51–58.

55 L. Lei, M. Tanishima, A. Goto and H. Kaji, *Polymers*, 2014, **6**, 860–872.

56 C.-G. Wang and A. Goto, *J. Am. Chem. Soc.*, 2017, **139**, 10551–10560.

57 H. Xu, C.-G. Wang, Y. Lu and A. Goto, *Macromolecules*, 2019, **52**, 2156–2163.

58 W. Mao, C.-G. Wang, Y. Lu, W. Faustinelie and A. Goto, *Polym. Chem.*, 2020, **11**, 53–60.

59 W. J. Lautenberger, E. N. Jones and J. G. Miller, *J. Am. Chem. Soc.*, 1968, **90**, 1110–1115.

60 L. Lei, M. Tanishima, A. Goto, H. Kaji, Y. Yamaguchi, H. Komatsu, T. Jitsukawa and M. Miyamoto, *Macromolecules*, 2014, **47**, 6610–6618.

61 P. Lacroix-Desmazes, R. Severac and B. Boutevin, *Macromolecules*, 2005, **38**, 6299–6309.

62 L. Xiao, K. Sakakibara, Y. Tsujii and A. Goto, *Macromolecules*, 2017, **50**, 1882–1891.

63 X. Liu, Q. Xu, L. Zhang, Z. Cheng and X. Zhu, *Polym. Chem.*, 2017, **8**, 2538–2551.

64 Q. Xu, C. Tian, L. Zhang, Z. Cheng and X. Zhu, *Macromol. Rapid Commun.*, 2019, **40**, 1800327.

65 B. Guo, L. Hou, Y. Li and L. Xiao, *Polymer*, 2020, **189**, 122201.

66 S. Dadashi-Silab, G. Szczepaniak, S. Lathwal and K. Matyjaszewski, *Polym. Chem.*, 2020, **11**, 843–848.

67 C.-G. Wang, H. W. Yong and A. Goto, *ACS Appl. Mater. Interfaces*, 2019, **11**, 14478–14484.

68 K. Hu, J. Sarkar, J. Zheng, Y. H. M. Lim and A. Goto, *Macromol. Rapid Commun.*, 2020, **41**, 2000075.

69 C. C. Robertson, R. N. Perutz, L. Brammer and C. A. Hunter, *Chem. Sci.*, 2014, **5**, 4179–4183.

70 K. E. B. Doncom, L. D. Blackman, D. B. Wright, M. I. Gibson and R. K. O'Reilly, *Chem. Soc. Rev.*, 2017, **46**, 4119–4134.

71 D. T. Gentekos, R. J. Sifri and B. P. Fors, *Nat. Rev. Mater.*, 2019, **4**, 761–774.

72 R. Whitfield, N. P. Truong, D. Messmer, K. Parkatzidis, M. Rolland and A. Anastasaki, *Chem. Sci.*, 2019, **10**, 8724–8734.

73 N. Corrigan, A. Almasri, W. Taillades, J. Xu and C. Boyer, *Macromolecules*, 2017, **50**, 8438–8448.

74 D. T. Gentekos, J. Jia, E. S. Tirado, K. P. Barteau, D.-M. Smilgies, R. A. DiStasio and B. P. Fors, *J. Am. Chem. Soc.*, 2018, **140**, 4639–4648.

75 M. Rubens and T. Junkers, *Polym. Chem.*, 2019, **10**, 6315–6323.

76 R. Whitfield, K. Parkatzidis, M. Rolland, N. P. Truong and A. Anastasaki, *Angew. Chem., Int. Ed.*, 2019, **58**, 13323–13328.

77 X. Liu, C.-G. Wang and A. Goto, *Angew. Chem., Int. Ed.*, 2019, **58**, 5598–5603.

78 M. Tanishima, A. Goto, L. Lei, A. Ohtsuki, H. Kaji, A. Nomura, Y. Tsujii, Y. Yamaguchi, H. Komatsu and M. Miyamoto, *Polymers*, 2014, **6**, 311–326.

79 J. Zheng, C.-G. Wang, Y. Yamaguchi, M. Miyamoto and A. Goto, *Angew. Chem., Int. Ed.*, 2018, **57**, 1552–1556.

80 J. Zheng, C. Chen and A. Goto, *Angew. Chem., Int. Ed.*, 2020, **59**, 1941–1949.

81 Y. Ge, C. Chen, X. M. Sim, J. Zheng and A. Goto, *Macromol. Rapid Commun.*, 2020, **41**, 1900623.

82 H. Yang, Z. Wang, Y. Zheng, W. Huang, X. Xue and B. Jiang, *Polym. Chem.*, 2017, **8**, 2137–2144.

83 H. Yang, Z. Wang, L. Cao, W. Huang, Q. Jiang, X. Xue, Y. Song and B. Jiang, *Polym. Chem.*, 2017, **8**, 6844–6852.

84 J. J. Chang, L. Xiao, C.-G. Wang, H. Niino, S. Chatani and A. Goto, *Polym. Chem.*, 2018, **9**, 4848–4855.

85 J. J. Chang, H. Niino, S. Chatani and A. Goto, *Polym. Chem.*, 2019, **10**, 5617–5625.

86 M. A. Tasdelen, M. U. Kahveci and Y. Yagci, *Prog. Polym. Sci.*, 2011, **36**, 455–567.

87 A. Anastasaki, J. Willenbacher, C. Fleischmann, W. R. Gutekunsta and C. J. Hawker, *Polym. Chem.*, 2017, **8**, 689–697.

88 C. Chen, L. Xiao and A. Goto, *Macromolecules*, 2016, **49**, 9425–9440.

89 C. Chen, C. G. Wang, L. Xiao and A. Goto, *Chem. Commun.*, 2018, **54**, 13738–13741.

90 C. Chen, C.-G. Wang, W. Guan and A. Goto, *Polym. Chem.*, 2019, **10**, 5913–5919.

91 C.-G. Wang, A. M. L. Chong, Y. Lu, X. Liu and A. Goto, *Chem. – Eur. J.*, 2019, **25**, 13025–13029.

92 P. L. Golas and K. Matyjaszewski, *Chem. Soc. Rev.*, 2010, **39**, 1338–1354.

93 S. Yamago and Y. Nakamura, *Polymer*, 2013, **54**, 981–994.

94 M. Chen, M. Zhong and J. A. Johnson, *Chem. Rev.*, 2016, **116**, 10167–10211.

95 X. Pan, M. A. Tasdelen, J. Laun, T. Junker, Y. Yagci and K. Matyjaszewski, *Prog. Polym. Sci.*, 2016, **62**, 73–125.

96 N. Corrigan, J. Yeow, P. Judzewitsch and C. Boyer, *Angew. Chem.*, 2019, **58**, 5170–5189.

97 N. J. Treat, H. Sprafke, J. W. Kramer, P. G. Clark, B. E. Barton, J. R. de Alaniz, B. P. Fors and C. J. Hawker, *J. Am. Chem. Soc.*, 2014, **136**, 16096–16101.

98 X. Pan, M. Lamson, J. Yan and K. Matyjaszewski, *ACS Macro Lett.*, 2015, **4**, 192–196.

99 S. Shanmugam, J. Xu and C. Boyer, *J. Am. Chem. Soc.*, 2015, **137**, 9174–9185.

100 M. Chen, M. J. MacLeod and J. A. Johnson, *ACS Macro Lett.*, 2015, **4**, 566–569.

101 J. C. Theriot, C. H. Lim, H. Yang, M. D. Ryan, C. B. Musgrave and G. M. Miyake, *Science*, 2016, **352**, 1082–1086.

102 A. Allushi, C. Kutahya, C. Aydogan, J. Kreutzer, G. Yilmaz and Y. Yagci, *Polym. Chem.*, 2017, **8**, 1972–1977.

103 A. Ohtsuki, L. Lei, M. Tanishima, A. Goto and H. Kaji, *J. Am. Chem. Soc.*, 2015, **137**, 5610–5617.

104 X. Liu, L. Zhang, Z. Cheng and X. Zhu, *Polym. Chem.*, 2016, **7**, 3576–3588.

105 X. Liu, L. Zhang, Z. Cheng and X. Zhu, *Chem. Commun.*, 2016, **52**, 10850–10853.

106 C. Tian, P. Wang, Y. Ni, L. Zhang, Z. Cheng and X. Zhu, *Angew. Chem., Int. Ed.*, 2020, **59**, 3910–3916.

107 Y. Ni, C. Tian, L. Zhang, Z. Cheng and X. Zhu, *ACS Macro Lett.*, 2019, **8**, 1419–1425.

108 F. Li, W. Yang, M. Li and L. Lei, *Polym. Chem.*, 2019, **10**, 3996–4005.

109 M. Yorizane, T. Nagasuga, Y. Kitayama, A. Tanaka, H. Minami, A. Goto, T. Fukuda and M. Okubo, *Macromolecules*, 2010, **43**, 8703–8705.

110 T. Kuroda, A. Tanaka, T. Taniyama, H. Minami, A. Goto, T. Fukuda and M. Okubo, *Polymer*, 2012, **53**, 1212–1218.

111 Y. Mai and A. Eisenberg, *Chem. Soc. Rev.*, 2012, **41**, 5969–5985.

112 M. J. Monteiro and M. F. Cunningham, *Macromolecules*, 2012, **45**, 4939–4957.

113 P. B. Zetterlund, S. C. Thickett, S. Perrier, E. Bourgeat-Lami and M. Lansalot, *Chem. Rev.*, 2015, **115**, 9745–9800.

114 N. J. W. Penfold, J. Yeow, C. Boyer and S. P. Armes, *ACS Macro Lett.*, 2019, **8**, 1029–1054.

115 F. D'Agosto, J. Rieger and M. Lansalot, *Angew. Chem.*, 2020, **59**, 2–27.

116 C. Liu, C.-Y. Hong and C.-Y. Pan, *Polym. Chem.*, 2020, **11**, 3673–3689.

117 J. Sarkar, L. Xiao, A. W. Jackson, A. M. van Herk and A. Goto, *Polym. Chem.*, 2018, **9**, 4900–4907.

118 J. Sarkar, A. W. Jackson, A. M. van Herk and A. Goto, *Polym. Chem.*, 2020, **11**, 3904–3912.

119 J. Zheng and A. Goto, *Polym. Chem.*, 2020, **11**, 3987–3993.

120 J. Yan, M. R. Bockstaller and K. Matyjaszewski, *Prog. Polym. Sci.*, 2020, **100**, 101180.

121 J. O. Zoppe, N. C. Ataman, P. Mocny, J. Wang, J. Moraes and H.-A. Klok, *Chem. Rev.*, 2017, **117**, 1105–1318.

122 Y. Tsujii, K. Ohno, S. Yamamoto, A. Goto and T. Fukuda, *Adv. Polym. Sci.*, 2006, **197**, 1–45.

123 K. Jung, N. Corrigan, M. Ciftci, J. Xu, S. E. Seo, C. J. Hawker and C. Boyer, *Adv. Mater.*, 2019, 1903850.

124 T. Chen, I. Amin and R. Jordan, *Chem. Soc. Rev.*, 2012, **41**, 3280–3296.

125 C.-G. Wang, C. Chen, K. Sakakibara, Y. Tsujii and A. Goto, *Angew. Chem., Int. Ed.*, 2018, **57**, 13504–13508.

126 X. M. Sim, C.-G. Wang, X. Liu and A. Goto, *ACS Appl. Mater. Interfaces*, 2020, **12**, 28711–28719.

127 S. N. Vouyiouka, E. K. Karakatsani and C. D. Papaspyrides, *Prog. Polym. Sci.*, 2005, **30**, 10–37.

128 R. Mohanrao, K. Hema and K. M. Sureshan, *Nat. Commun.*, 2020, **11**, 865.

129 I. E. Claassens, L. J. Barbour and D. A. Haynes, *J. Am. Chem. Soc.*, 2019, **141**, 11425–11429.

130 R. Z. Lange, G. Hofer, T. Weber and A. D. Schlüter, *J. Am. Chem. Soc.*, 2017, **139**, 2053–2059.

131 H. T. Le, C.-G. Wang and A. Goto, *Angew. Chem., Int. Ed.*, 2020, **59**, 9360–9364.